SmpB: A Protein that Binds to Double-Stranded Segments in tmRNA and tRNA†

Jacek Wower,‡ Christian W. Zwieb,§ David W. Hoffman,|| and Iwona K. Wower*,‡

Department of Animal Sciences, Program in Cell and Molecular Biosciences, Auburn University, Auburn, Alabama 36849-5415, Department of Molecular Biology, The University of Texas Health Science Center at Tyler, 11937 US Highway 271, Tyler, Texas 75708-3154, and Department of Chemistry and Biochemistry Institute for Cellular and Molecular Biology, University of Texas at Austin, Austin, Texas 78712

Received February 15, 2002; Revised Manuscript Received April 22, 2002

ABSTRACT: Binding of the SmpB protein to tmRNA is essential for trans-translation, a process that facilitates peptide tagging of incompletely synthesized proteins. We have used three experimental approaches to study these interactions in vitro. Gel mobility shift assays demonstrated that tmRNA(Δ90−299), a truncated tmRNA derivative lacking pseudoknots 2−4, has the same affinity for the *Escherichia coli* and *Aquifex aeolicus* SmpB proteins as the intact *E. coli* tmRNA. These interactions can be challenged by double-stranded RNAs such as tRNAs and 5S rRNA and are abolished by removal of 24 amino acids from the C-terminus of the *A. aeolicus* protein. A combination of enzymatic probing and UV-induced cross-linking showed that three SmpB molecules can bind to a single tmRNA(Δ90−299) and tRNA molecule. Irradiation of *E. coli* tmRNA and yeast $tRNA^{Phe}$ bound to a single SmpB molecule with UV light induced cross-links to residues C343 and m^1A48, respectively, in their T-loops and to their 3′ terminal adenosines. These findings indicate that the acceptor-T arm constitutes the primary SmpB binding site in both tmRNA and tRNA. The remaining two SmpB molecules associate with the anticodon stem-like region of tmRNA and the anticodon arm of tRNAs. As the T and anticodon loops are dispensable for SmpB binding, it seems that SmpB recognizes double helical segments in both tmRNA and tRNA molecules. Although these interactions involve analogous elements in both molecules, their different effects on aminoacylation appear to reflect subtle structural differences between the tRNA-like domain of tmRNA and tRNA.

Trans-translation is an important quality control step in protein synthesis (for reviews see, *1*−*3*). This process tags defective proteins for which synthesis was prematurely terminated with short peptide tags recognized by many housekeeping proteases, and thus it facilitates their degradation. Several lines of evidence indicate that trans-translation is activated when ribosomes are stalled either on the 3′ end of damaged mRNAs or at mRNA segments rich in rare codons (*4*−*6*). The key component of the trans-translational apparatus is tmRNA[1] (originally known as 10Sa RNA), a small, stable RNA molecule encoded by the *ssrA* gene. This molecule is ubiquitous in bacteria (*7*). Analogues of tmRNA have also been found in the genomes of certain chloroplasts and mitochondria. Although tmRNA is not essential for many bacteria, its presence seems to be advantageous for their survival (*8*).

Extensive in vitro and in silico analyses of tmRNA molecules revealed that their structures consist of three distinct features (*9*−*11*). The 3′ and 5′ terminal sequences of all known tmRNAs form a tRNA-like domain that is connected to a pseudoknot-rich domain embracing the mRNA-like domain ending with a stop codon tandem. The mRNA domain of tmRNA encodes 10−27 amino acid-long peptides having at their C-termini nonpolar (Y/A)A(L/V)-AA sequences recognized by the HlfB, ClpXP, ClpAP, and Tsp proteases (*4*).

Despite a significant reduction of the D domain (the equivalent of the D arm in tRNAs), the three-dimensional folding of the tRNA-like domain closely resembles the L-shaped structure of canonical tRNAs (*12*). This model is supported by recent transient electric birefringence measurements of the *Escherichia coli* tmRNA, which showed that the interstem angle may be 10−20° larger than the corresponding angle in the crystal structure of yeast $tRNA^{Phe}$ (*13*). Moreover, recent mutagenesis studies of the *E. coli* tmRNA carried out by Hanava-Suetsugu et al. (*14*) confirmed the base-pairing between 19GA20 and 333GA334 suggested earlier by Zwieb et al. (*12*). While the present three-dimensional model of tmRNA is rather extended, a number of forthcoming data indicate that the pseudoknot-rich domain is tightly packed (*15*, *16*).

Our present knowledge of the tmRNA structure is consistent with many elements of the original scheme of trans-

† This work was supported by National Institute of Health Grant GM58267 to J.W.

* Corresponding author. Address: Department of Animal Sciences, Program in Cell and Molecular Biosciences, Auburn University, 209 Upchurch Hall, Auburn, AL 36849-5415. Tel: (334) 844-1509. Fax: (334) 844-1519. E-mail: iwower@acesag.auburn.edu.

‡ Auburn University

§ The University of Texas Health Science Center at Tyler.

|| University of Texas at Austin

[1] Abbreviations: tmRNA, transfer-messenger RNA; tmRNA(Δ90−299), truncated tmRNA derivative lacking nucleotides 90−299; $SmpB_{His}$, *E. coli* SmpB protein tagged with six histidines at its 3′ terminus; $2N_3A$, 2-azidoadenosine; rRNA, ribosomal RNA.

10.1021/bi0201365 CCC: $22.00
Published on Web 06/19/2002

translation suggested by Keiler et al. (*4*). According to this proposal, tmRNA binds to the A site of the stalled ribosomes, accepts the peptidyl moiety from the P site-bound tRNA, and makes its mRNA domain available to canonical tRNAs that mediate the synthesis of the peptide tag until the stop codons of tmRNA are reached. Although tmRNA is essential for trans-translation, many in vitro and in vivo studies have demonstrated that the functions of tmRNA have to be supported by proteins. Some of these proteins, including ATP/CTP tRNA nucleotidyl transferase and alanyl-tRNA synthetase, are well-known components of the translational apparatus that specifically interact with the acceptor-T arm of in tRNA (*17*, *18*). Formation of the ternary complex between the *E. coli* alanyl-tmRNA, elongation factor Tu (EF-Tu), and GTP has been demonstrated by Barends et al. (*19*). As in tRNA, EF-Tu binds exclusively to the acceptor-T arm of the tRNA-like domain in the *E. coli* tmRNA (*20*). However, unusual aminoacylation- and GTP-independent interactions between tmRNA and EF-Tu proposed recently by Zvereva et al. (*21*) may involve other parts of the tmRNA molecule. Moreover, it has been demonstrated that tmRNA forms complexes with ribosomal protein S1 and that this protein is required for binding of tmRNA to 30S and 70S ribosomal particles (*22*). In *E. coli*, the interactions with protein S1 are limited to the mRNA and pseudoknot-rich domains in tmRNA.

Recent studies have identified three additional proteins—phosphoribosyl pyrophosphate synthase, RNase R, and a protein of unknown function encoded by the *yfbG* gene—capable of forming complexes with tmRNA (*23*). These proteins, however, are less likely to be involved in trans-translation, as efficient protein tagging could be induced in the cell-free translation system consisting only of purified ribosomes, alanyl-tRNA synthetase, elongation factors, SmpB protein, tRNAs, and tmRNA (*24*).

Deletion of the *smpB* gene results in growth defects characteristic of *E. coli* ssrA mutants, suggesting the involvement of SmpB protein in trans-translation (*25*−*27*). Although *smpB* genes have been found in all sequenced prokaryotic genomes, so far only SmpB proteins from *Aquifex aeolicus* and *E. coli* have been investigated. An examination of SmpB protein from *A. aeolicus* by multidimensional NMR methods revealed that it consists of a barrel of antiparallel β strands and three helices (*28*). The same three-dimensional folding is likely to be adopted by other SmpB proteins, as an analysis of their sequences shows a very high degree of amino acid conservation. Because conserved basic amino acids cluster on the opposite sides of the SmpB protein, Dong et al. (*28*) suggested that the SmpB protein might have two RNA-binding sites.

According to Karzai et al. (*27*), SmpB protein is required for the stable association of tmRNA with 70S ribosomes. However, even after the dissociation of ribosomes into subunits, the SmpB protein remains associated with tmRNA (*1*). Purified SmpB binds to tmRNA with high affinity (*27*). The binding of SmpB protein to tmRNA does not affect the interactions of the latter with either ribosomal protein S1 or EF-Tu (*20*). In contrast, SmpB association with tmRNA seems to stimulate the aminoacylation of tmRNA by alanyl-tRNA synthetase, which, like EF-Tu, is known to specifically recognize the acceptor-T arm in canonical $tRNA^{Ala}$. Since all the information related to SmpB function comes from studies of the *E. coli* protein and only the structure of *A. aeolicus* SmpB protein is known, to better understand the role SmpB plays in trans-translation, we cross-examined the interactions between *E. coli* tmRNA and SmpB proteins from both bacteria.

MATERIALS AND METHODS

Materials. The sources of enzymes, radioactively labeled nucleotides, and other biological materials are the same as those given in Wower et al. (*28*). Cloning, expression, and purification of SmpB protein from *Aquifex aeolicus* and its truncated form SmpB(Δ134−157), which lacks 24 C-terminal amino acids, is described in Dong et al. (*28*).

Preparation of tmRNAs, tRNAs, and 5S rRNA. Cloning, synthesis, and purification of *E. coli* tmRNA and its truncated derivative tmRNA(Δ90−299) is described in Wower et al. (*22*).

The unmodified *E. coli* $tRNA(UGC)^{Ala}$ was prepared by in vitro transcription of the plasmid pALA119 kindly provided by Dr. J. Horowitz (*30*). Acceptor-T arm analogues of tmRNA and tRNA molecules were prepared by transcription of single-stranded DNA templates according to Milligan et al. (*31*).

5S rRNA was extracted from *E. coli* strain MRE 600 according to Monier and Feunteun (*32*). Following 3′-end labeling with [^{32}P]Cp, 5S RNA was purified by electrophoresis on a 12% denaturing polyacrylamide gel and renatured as described by Douthwaite and Garrett (*33*).

The 3′- and 5′-^{32}P-labeled RNAs were prepared as described by England et al. (*34*) and Silberklang et al. (*35*), respectively. Alternatively, the tmRNA, tRNA, and acceptor-T arm were labeled at their 3′ ends by the −CCA replacement as described earlier (*22*).

Cloning, Expression, and Purification of the His-Tagged E. coli Protein SmpB. The coding sequence of the *smpB* gene was amplified by PCR from the *E. coli* genomic DNA using an pstream primer (5′-AAATAATTTTGTTTAACTTT-AAGAAGGAGATATACATATGACGAAGAAAAAAGC-ACATAAAC-3′) and a downstream primer (5′-CAGTG-GTGGTGGTGGTGGTGCTCGAGACGGTGGGCGTTTTT-CATGATA-3′). The resulting DNA fragment was digested with restriction enzymes *Nde*I and *Xho*I and cloned into plasmid pET-23a (Novagen) to yield plasmid pET*smpB*. This plasmid encoded protein SmpB was tagged at its C-terminus with six histidine residues and named $SmpB_{His}$. Protein $SmpB_{His}$ was overexpressed in *E. coli* strain BL21(DE3)-pLysS transformed with pET*smpB*, purified on Ni^{2+}−NTA−agarose (Qiagen) under denaturing conditions, and dialyzed against buffer containing 50 mM MES (pH 6.5), 200 mM KCl, 5 mM 2-mercaptoethanol, and 10% glycerol. This procedure yields $SmpB_{His}$ protein that is >98% pure.

Gel Mobility Shift Assay. K_d values for SmpB:RNA complex formation were measured as in Wower et al. (*22*). Binding of the SmpB protein to RNA ligands was carried out in a binding buffer containing either 50 mM MES (pH 6.5) or 50 mM Tris-HCl (pH 7.5), 200 mM KCl, 5% glycerol, 5 mM 2-mercaptoethanol, 0.01% NP-40, and 0.1 mg/mL bovine serum albumin (*27*). The specificity of the interaction between tmRNA and SmpB proteins was investigated by competition assays as described earlier (*22*). Unlabeled *E. coli* tmRNA, total *E. coli* tRNA, and 40−80-

nucleotide-long poly(U) were used as competitors. Binding of SmpB proteins to RNA ligands was visualized and quantified using PhosphoImager SI and ImageQuant 1.2 software (Molecular Dynamics).

Enzymatic Footprinting of SmpB:RNA Complexes. Conditions for partial nuclease digestions of tmRNA and tRNA species in the absence or the presence of SmpB proteins were adopted from Christiansen et al. (*36*). The experiments were conducted with 1 μM RNAs at ratios of protein to RNA varying from 0.1:1 to 10:1. These concentrations should ensure the formation of the complex, since the K_d of *E. coli* SmpB protein for tmRNA is 20−100 nM (*20, 27*).

UV-Induced Cross-Linking of the SmpB Protein to E. coli tmRNA(Δ90−299) and Yeast tRNA^{Phe}. Cross-linking was accomplished by irradiating 3′-^{32}P-labeled RNA:SmpB complexes for 10 min at 0 °C with four RPR-2540-Å lamps as described by Wower et al. (*37*). Concentrations of RNAs and the ratios of protein to RNA were as in enzymatic footprinting experiments.

Analysis of Covalent tmRNA−SmpB and tRNA−SmpB Complexes. Sites of cross-linking in tmRNA were determined by digestion of cross-linked tmRNA(Δ90−299)−SmpB complexes with RNase H in the presence of selected oligodeoxyribonucleotides in combination with primer extension using reverse transcriptase as described by Zwieb et al. (*12*). To generate precise cleavages in the T loop of tmRNA, we used two chimeric oligonucleotides denoted as "oligo a" [deoxy(GAAC)2′-Ome-(CCCGCGUCCGAAAUU)-riboC] and "oligo b" [deoxy(CCGC)-2′-Ome-(GUCCGAAAUU)-riboC] complementary to nucleotides 325−343 and 325−339 in the *E. coli* tmRNA. "Oligo c" was deoxy-CCTCGGTACTA-CATG complementary to nucleotides 304−318. Primer extension analysis of the T arm of the cross-linked tmRNA-(Δ90−299)−SmpB complexes was carried out with a dodecadeoxyribonucleotide complementary to the 3′ end of the *E. coli* tmRNA (residues 352−363).

Sites of cross-linking in tRNA were determined as described by Abdurashidova et al. (*38*). In this approach, purified 3′-^{32}P-labeled tRNA−SmpB complexes are subjected to limited alkaline hydrolysis. The hydrolysate is extracted with phenol and the oligonucleotides that partition into the aqueous phase are analyzed on a 20% polyacrylamide gel in 100 mM Tris-100 mM H_3BO_4 (pH 8.3) containing 2.5 mM EDTA and 8 M urea.

Affinity Labeling of the SmpB Protein by 2N$_3$A-Substituted tmRNA and tRNA Derivatives. 2-Azidoadenosine 3′,5′-bisphosphate (p2N$_3$Ap) was synthesized and ^{32}P-labeled as described by Sylvers et al. (*39*). 2-Azidoadenosine 3′,5′-[5′-^{32}P]bisphosphate was incorporated into the 3′-position of yeast tRNA^{Phe} truncated by either one or four nucleotides at its 3′-terminus to yield [5′-^{32}P](2N$_3$A76)tRNA^{Phe} and [5′-^{32}P](2N$_3$A76)tRNA^{Phe} according to the procedure described earlier (*29*, *39*). The same approach was used to prepare [5′-^{32}P](2N$_3$A363)tmRNA(Δ90−299), a photoreactive tmRNA derivative containing 2N$_3$A at its 3′ terminus. Noncovalent binding of photoreactive RNA derivatives to SmpB proteins was performed as described in the gel mobility shift assay (see above). Complexes were then irradiated for 2 min at 4 °C with 300-nm UV light (*37*). Cross-linked (2N$_3$A)tmRNA-(Δ90−299)−SmpB and (2N$_3$A)tRNA−SmpB complexes were isolated on 6% and 10% polyacrylamide gels in Tricine-SDS buffer (*40*).

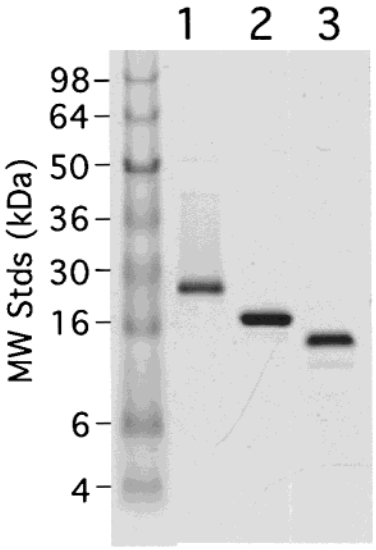

FIGURE 1: SDS−PAGE of SmpB proteins. Lane 1: His-tagged SmpB protein from *E. coli*. Lane 2: An intact SmpB protein from *A. aeolicus*. Lane 3: *A. aeolicus* SmpB protein lacking 24 amino acids on its C-terminus. Molecular mass markers are shown on the left.

RESULTS

Binding of E. coli and A. aeolicus SmpB Proteins to E. coli tmRNA, Various tRNAs, and Their Truncated Derivatives. Wild-type SmpB protein from *E. coli* was shown to bind to unmodified *E. coli* tmRNA with K_d of 20−100 nM (*20, 27*). To study this ribonucleoprotein complex, we prepared SmpB$_{His}$ protein, a derivative of the *E. coli* SmpB protein tagged at its C-terminus with six histidine residues and isolated an intact SmpB protein from *A. aeolicus* and its truncated derivative SmpB(Δ134−157) lacking 24 C-terminal amino acids (Figure 1). Unlike *E. coli* SmpB, which tend to aggregate at concentrations >100 μM especially at a pH greater than 7.5, the *A. aeolicus* protein remained soluble over a wide range of concentrations when stored at pH 6.5. Gel mobility shift assays demonstrated that the binding of *E. coli* SmpB$_{His}$ and intact *A. aeolicus* SmpB proteins to both the intact unmodified *E. coli* tmRNA and its truncated derivative tmRNA(Δ90−299) was saturable with half-maximal binding at a free protein concentration of ∼100 nM. The SmpB(Δ134−157) protein failed to bind tmRNA. Since deletion of residues 90−299 does not affect the integrity of the remaining fragment of tmRNA (*12*), these experiments indicated that the region encompassing the mRNA-like domain and pseudoknots pk2, pk3, and pk4 is not important for interactions with the SmpB protein (see Figure 2a). Moreover, since removal of a peptide encompassing 134-RRELKEKAMKRELEREFKGKIHL-157 from *A. aeolicus* SmpB has no impact on its three-dimensional folding (*28*), the C-terminal sequence of the SmpB protein is likely to be directly involved in binding to the tmRNA molecule.

Testing the specificity of the interactions between tmRNA and the SmpB proteins, we found that, unlike poly(U) and poly(A), the *E. coli* 5S rRNA and total *E. coli* tRNA, when added to the binding mixture simultaneously with ^{32}P-labeled tmRNA(Δ90−299), inhibit binding of the latter molecule to SmpB proteins (Figure 3a). Given that *E. coli* 5S RNA and tRNAs are structurally quite different, this observation

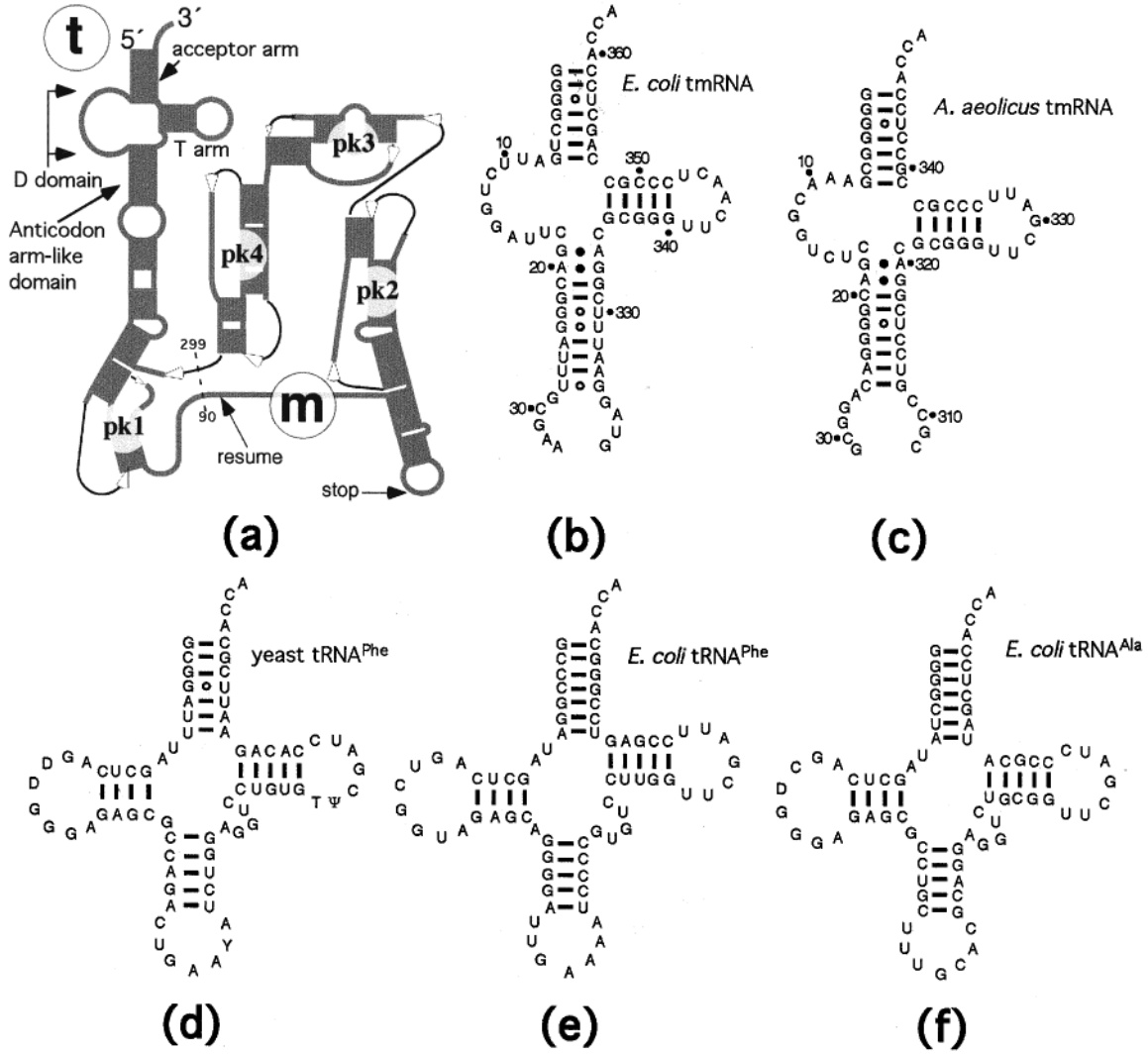

FIGURE 2: RNA ligands of SmpB proteins. (a) Schematic representation of the secondary structure of the *E. coli* tmRNA. The mRNA, tRNA-like domains, and pseudoknots are marked m, t, and pk, respectively. (b and c) Secondary structures of tRNA-like domains of *E. coli* and *A. aeolicus* tmRNAs. (d−f) Cloverleaf structures of yeast $tRNA^{Phe}$, and *E. coli* $tRNA^{Phe}$, and $tRNA^{Ala}$.

suggested that SmpB may recognize common features of the RNA molecules, such as double-stranded regions.

The competition effect observed in the presence of total *E. coli* tRNA is at odds with an earlier report that the total yeast tRNA does not compete well with tmRNA for the wild-type SmpB (*27*). Additional gel mobility shift assays showed that yeast $tRNA^{Phe}$, *E. coli* $tRNA^{Phe}$, $tRNA^{Al,a}$ and $tRNA^{Glu}$, as well as *E. coli* 5S rRNA, can bind to both the *E. coli* and *A. aeolicus* SmpB proteins, with K_d ranging from ∼100 nM for *E. coli* $tRNA^{Ala}$ to ∼400 nM for yeast $tRNA^{Phe}$ (for example, see Figure 3b). Since intracellular concentrations of tRNA isoacceptors vary from 2 to 25 μM, SmpB protein is likely to bind to tRNA molecules in vivo (*41*).

Enzymatic Footprinting of SmpB−RNA Complexes. To map the segments of *E. coli* tmRNA(Δ90−299) and yeast $tRNA^{Phe}$ that are in contact with SmpB, we used RNases V1, T1, and nuclease S1, which have been utilized widely to examine, for example, tRNA:aminoacyl-tRNA synthetase and aminoacyl-tRNA:EF-Tu:GTP complexes (*42*, *43*).

Figure 4 displays examples of footprinting experiments carried out with both 3′- and 5′-^{32}P-labeled *E. coli* tmRNA(Δ90−299) and yeast $tRNA^{Phe}$ in the presence of increasing *E. coli* $SmpB_{His}$ concentrations (up to 1 μM). Consistent with their known enzymatic specificities, RNase V1 nicked RNA segments with an approximately helical conformation (*44*), while nuclease S1 cleaved exclusively single-stranded RNA (*45*). In tRNA, RNase T1 cleaved after non-base-paired guanosine residues (*46*). However, in tmRNA(Δ90−299), unexpectedly but reproducibly, RNase T1 also cleaved phosphodiester bonds after C residues at positions 331, 349, and 350 (Figure 4b). According to the present model of tRNA-like domain structure, these residues are located in helical sections. Similar patterns were observed when footprinting experiments were carried out in the presence of the *A. aeolicus* SmpB protein (not shown).

Phosphodiester bonds protected by SmpB protein from RNase cleavage clustered primarily in the double-helical regions and T loops of *E. coli* tmRNA(Δ90−299) and yeast $tRNA^{Phe}$ (Figures 4f and 4g). At large excess of SmpB proteins over tmRNA, protections were also visible in pseudoknot pk1. No useful data on SmpB interactions with the D domain of tmRNA and the D loop of tRNA were provided by footprinting experiments because these RNA segments were not susceptible to nicking by nuclease S1 and RNase T1. Nevertheless, the data collected indicated that

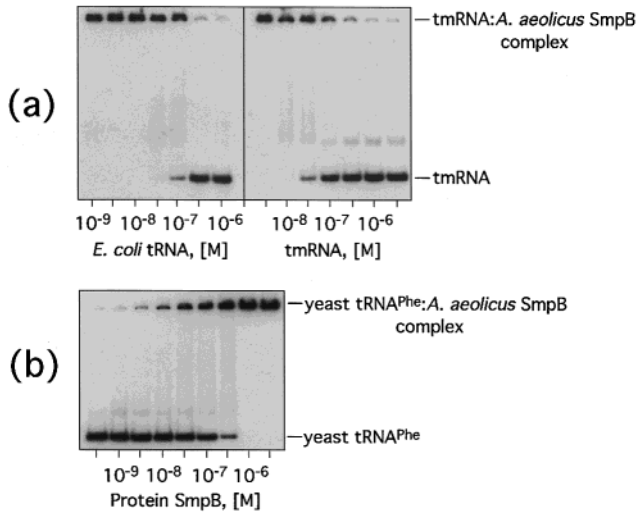

FIGURE 3: Gel mobility shift analysis of binding between SmpB proteins and their RNA ligands. (a) Competition for binding of 3′-^{32}P-labeled *E. coli* tmRNA to *A. aeolicus* SmpB protein by total *E. coli* tRNA (left) and *E. coli* tmRNA (right). Increasing concentrations of unlabeled competitor RNA, either a mixture of all *E. coli* tRNAs or tmRNA, were added to the binding reaction, which contained 10^{-9} M 3′-^{32}P-labeled *E. coli* tmRNA and 2.0×10^{-7} SmpB protein. (b) Titration of the 3′-^{32}P-labeled yeast tRNA^{Phe} (10^{-9} M) with the *A. aeolicus* SmpB protein.

the SmpB protein is able to make contact with a large portion of tmRNA(Δ90−299) and almost the entire tRNA molecule. Given that the SmpB protein is quite small and the length of its "core" does not exceed 51 Å, such extensive contacts cannot be elicited by a single protein molecule.

Cross-Links between tmRNA, tRNA, and SmpB Proteins. To gain further insight into the structure of the SmpB:tmRNA and SmpB:tRNA complexes, we irradiated them with near-UV light. Because UV-irradiation generates cross-links both within the RNA molecule and between RNA and proteins that are in close contact, this approach provides a straightforward means of studying both the three-dimensional folding of RNA molecules and the topography of ribonucleoprotein complexes (*47*).

Irradiation of equimolar mixtures of tmRNA(Δ90−299) and SmpB$_{His}$ and of yeast tRNA^{Phe} and SmpB$_{His}$ with 254 nm light yielded covalently bound tmRNA(Δ90−299)−SmpB$_{His}$ and tRNA−SmpB$_{His}$ complexes that could be readily separated from un-cross-linked RNA on SDS−Tricine polyacrylamide gels as shown in Figures 5a and 5b (lane 4 in each). Approximately 10−12% of tmRNA and tRNA species cross-linked to SmpB when UV irradiation was limited to 10 min (in order to avoid the formation of any significant amount of intra-RNA cross-links), particularly in tmRNA (*12*). No cross-linked species were observed in control reactions containing a 10-fold excess of nonlabeled total *E. coli* tRNAs and tmRNA (Figure 5a,b, lanes 5−12). When tmRNA(Δ90−299) and tRNAs were irradiated in the presence of increasing amounts of SmpB$_{His}$ protein (up to 10 molar excess over tmRNA and tRNA), gradual formation of two additional covalent RNA−protein complexes were observed on SDS−Tricine polyacrylamide gels (Figure 5a,b, lane 13 in each). The tmRNA−(SmpB)$_2$ and tRNA(SmpB)$_2$ complexes were clearly visible when the protein:RNA ratio in the binding mixture was close to 3. The tmRNA−(SmpB)$_3$ and tRNA(SmpB)$_3$ complexes began to form when the protein:RNA ratio in the binding mixture reached 8. These observations are congruent with the results of footprinting experiments, which suggested that more than one SmpB protein may be able to bind to each tmRNA(Δ90−299) and tRNA molecule.

Topography of Covalent tmRNA(Δ90−299)−SmpB$_{His}$ and tRNA^{Phe}−SmpB$_{His}$ Complexes. Two approaches were combined to identify the site(s) in tmRNA to which SmpB protein was cross-linked. Oligodeoxyribonucleotide-directed cleavage of tmRNA(Δ90−299) cross-linked to SmpB$_{His}$ protein with RNase H was used to identify cross-linked tmRNA segments (*47*). Cross-linked portions of tmRNA(Δ90−299) were then scanned by primer extension to identify cross-linked nucleotide(s) (*48*).

The gel-purified complexes containing only one 3′-^{32}P-labeled tmRNA(Δ90−299) and SmpB$_{His}$ molecule were digested with RNase H and oligodeoxyribonucleotides placed at increasing distances from the 3′ end (see Materials and Methods; Figure 6a). Although the elevated temperature required for annealing of oligonucleotides to tmRNA (55 °C) and its oligonucleotide-programmed degradation by RNase H (47 °C) caused a dissolution of approximately 50% of the complexes, such treatment yielded a well-defined set of 3′-^{32}P-labeled tmRNA fragments of varying length. The location of the cross-linked segment was mapped by comparing differences in the digestion patterns between un-cross-linked and cross-linked tmRNA(Δ90−299) (Figure 6b). The shortest tmRNA fragment covalently attached to SmpB protein was produced by RNase H in the presence of chimeric oligonucleotide oligo a, which facilitates precise cutting between residues 341−343. Thus, this RNase H analysis confined the cross-linked site to the 3′-terminal tmRNA segment encompassed by nucleotides 341−363. However, because RNase T1 digestion of both 3′-^{32}P-labeled un-cross-linked and cross-linked tmRNA(Δ90−299) released 3′-terminal octamer CUCCACCA, the site of the cross-linking could be delimited even further to positions 341−355 (not shown). This segment of tmRNA(Δ90−299) was scanned using a primer extension approach. To differentiate between photodamaged and cross-linked nucleotides, we also carried out control analyses on tmRNA(Δ90−299) species that had been UV-irradiated but not cross-linked. A single strong stop was observed at A344 (Figure 7a). Therefore, assuming that the arrest occurred at one residue 3′ of the cross-linked nucleotide, the result indicated that SmpB$_{His}$ was covalently attached to the C343 residue in *E. coli* tmRNA.

To determine which nucleotide(s) in yeast tRNA^{Phe} were cross-linked to SmpB$_{His}$, we used an approach described by Abdurashidova et al. (*38*). After using the RNase H approach to determine that the SmpB$_{His}$ protein was cross-linked to the 3′-half of the tRNA^{Phe} molecule, we subjected gel-purified covalent complexes of 3′-^{32}P-labeled yeast tRNA^{Phe} and SmpB$_{His}$ protein to limited alkaline hydrolysis and then extracted them with phenol. Protein-free oligonucleotides that partitioned into the aqueous phase were subjected to electrophoresis on a denaturing 20% polyacrylamide gel, along with the alkaline ladders derived from the un-irradiated and the UV-irradiated 3′-^{32}P-labeled yeast tRNA^{Phe} (Figure 7b, lane 4). The ladder obtained from the tRNA−protein complex contained no fragments over 18 residues in length, thus indicating that SmpB was cross-linked to the m^{1}A58 residue in the T loop of yeast tRNA^{Phe}.

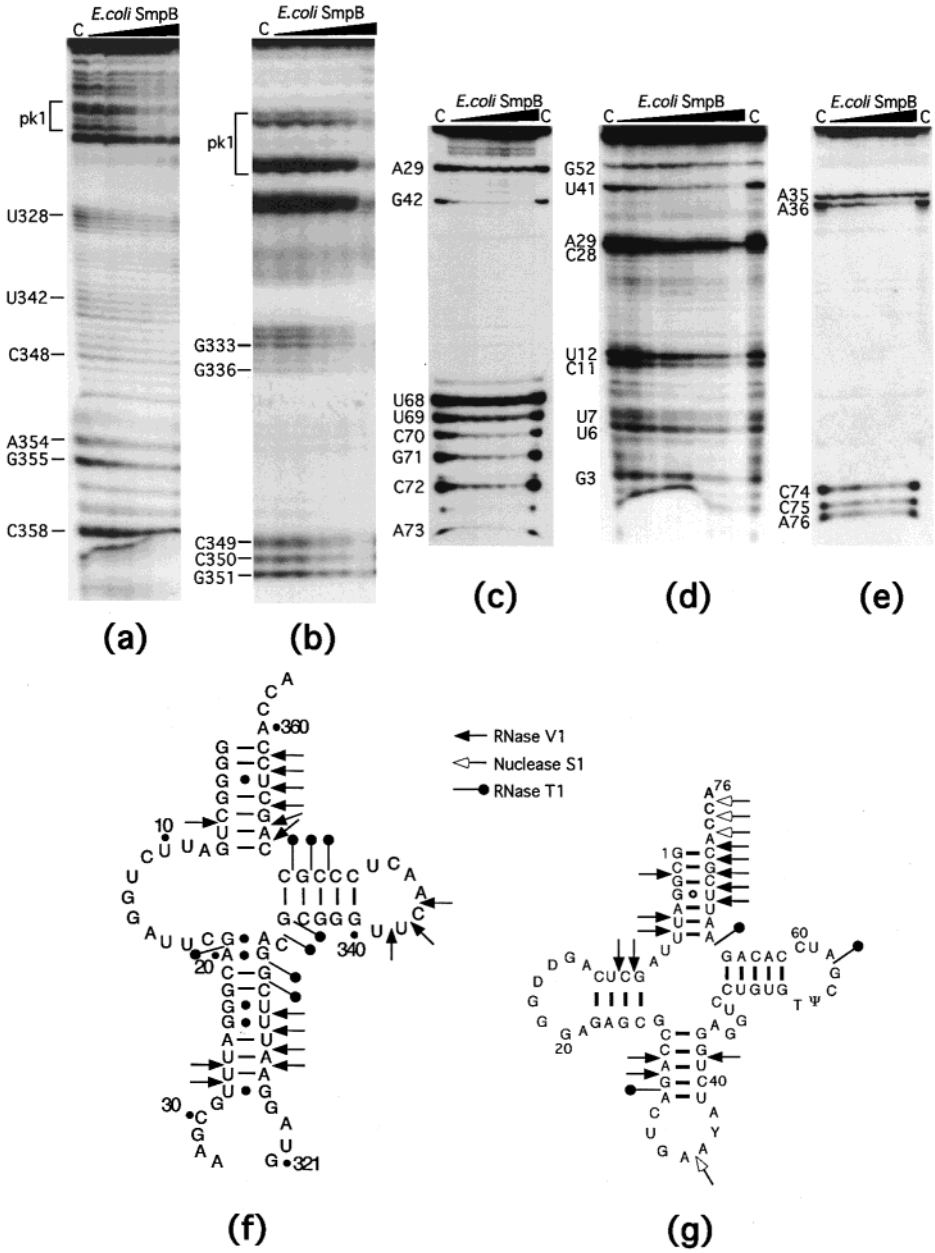

FIGURE 4: Enzymatic probing of tmRNA and tRNA bound to the *E. coli* SmpB protein. Upper panel: Examples of sequencing gels displaying the partial digestion of the *E. coli* tmRNA(Δ90−299)−$SmpB_{His}$ complexes with RNases V1 (a) and T1 (b) and yeast $tRNA^{Phe}$−SmpB complexes with RNase V1 (c and d) and nuclease S1 (e). The experiments were conducted with 1 μM RNAs. The protein:RNA ratio in analyzed complexes was gradually increased from 0.1 to 3.0. C denotes control digestions carried out in the absence of protein. Letters and numbers on the left sides of autoradiograms denote nucleotides adjacent to phosphodiester bonds protected by the bound protein. The region forming pseudoknot 1 is identified as pk1. Lower panel: Summary of nuclease cleavage sites in the tRNA-like domain of the *E. coli* tmRNA (f) and yeast $tRNA^{Phe}$ (g) protected by the SmpB protein.

RNase H analysis of cross-linked tmRNA(Δ90−299)−$(SmpB)_2$ and yeast $tRNA^{Phe}$−$(SmpB)_2$ complexes revealed that the second SmpB protein is covalently attached to segments encompassing nucleotides 330−335 in tmRNA and nucleotides 42−49 in tRNA (not shown). Further analysis identified m^7G46 as a site to which the second SmpB protein molecule is cross-linked in yeast $tRNA^{Phe}$ (Figure 7 b, lane 5).

Affinity Labeling of the SmpB Protein. Cross-linking of SmpB protein to the T loop in tmRNA and tRNA and the strong protection of their 3′ termini by SmpB protein indicated by footprinting with nuclease S1 suggested that the first SmpB molecule binds to the acceptor-T arm in both RNA species. To test this possibility, we replaced the 3′-terminal adenosines in tmRNA(Δ90−299) and yeast $tRNA^{Phe}$ with a photoreactive analogue, 2-azidoadenosine ($2N_3A$). The resulting ($2N_3A363$)tmRNA(Δ90−299) and ($2N_3A76$)-$tRNA^{Phe}$ were bound to $SmpB_{His}$ protein at a protein:RNA ratio of 0.9 and then irradiated with far-UV light. Such treatment, as we demonstrated in an earlier study, does not induce cross-links between unmodified RNA and bound proteins (*28*). Analysis of irradiated samples on SDS−Tricine polyacrylamide gel showed that approximately 8% of ($2N_3A363$)tmRNA(Δ90−299) and 10% of ($2N_3A76$)$tRNA^{Phe}$ cross-linked to the $SmpB_{His}$ protein (Figure 8). A similar efficiency was observed when affinity labeling was carried out with ($2N_3A73$)$tRNA^{Phe}$, a photoreactive yeast $tRNA^{Phe}$ derivative lacking the CCA terminus. The efficiency of

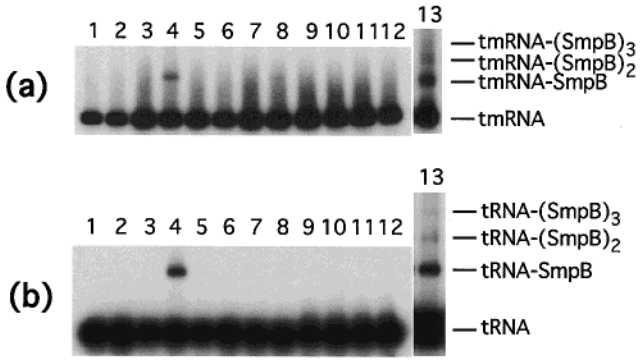

FIGURE 5: UV-induced cross-linking of the *E. coli* $SmpB_{His}$ protein to its RNA ligands. (a) Formation of covalent *E. coli* [^{32}P]tmRNA-(Δ90−299)−SmpB complexes. (Lane 1) Nonirradiated tmRNA-(Δ90−299), (lane 2) UV-irradiated tmRNA(Δ90−299), (lane 3) nonirradiated tmRNA(Δ90−299)−SmpB complexes, and (lane 4) UV-irradiated tmRNA(Δ90−299)−SmpB complexes. Lanes 5−8 and lanes 9−12 are the same as lanes 1−4 except for the presence of a 10-fold molar excess of unlabeled total *E. coli* tRNA and tmRNA, respectively. (Lane 13) Formation of covalent tmRNA-(Δ90−299)−SmpB complexes in the presence of 10-fold molar excess of the protein. (b) Formation of covalent yeast [^{32}P]-$tRNA^{Phe}$−SmpB complexes. (Lane 1) Nonirradiated $tRNA^{Phe}$, (lane 2) UV-irradiated $tRNA^{Phe}$, (lane 3) nonirradiated $tRNA^{Phe}$−SmpB complexes, and (lane 4) UV-irradiated $tRNA^{Phe}$−SmpB complexes. Lanes 5−8 and lanes 9−12 are the same as lanes 1−4 except for the presence of a 10-fold molar excess of unlabeled total *E. coli* tRNA and tmRNA, respectively. (Lane 13) Formation of covalent $tRNA^{Phe}$−SmpB complexes in the presence of a 10-fold molar excess of the protein.

SmpB labeling by both ($2N_3$A363)tmRNA(Δ90−299) and ($2N_3$A76)$tRNA^{Phe}$ increases slightly when 3-fold molar excess of protein over RNA is used. Because such treatment does not affect the mobility of the cross-linked RNA-protein complexes, affinity-labeling experiments indicate that only one SmpB molecule is able to bind to the acceptor stem of the tRNA-like domain of tmRNA and tRNA molecules.

Interactions of SmpB Proteins with Acceptor-T and Anticodon Arm Analogues. UV-induced cross-linking of equimolar SmpB−tRNA and SmpB−tRNA complexes and affinity labeling of SmpB protein by photoreactive tmRNA and tRNA derivatives demonstrated that the first SmpB protein that binds to both RNA molecules makes contact with 3′-terminal and T loop regions of the acceptor-T arm. To test whether the synthetic acceptor-T arm fragment of tmRNA is able to interact with SmpB proteins, we used a gel mobility shift assay. As shown in Figure 9a, the binding of *E. coli* $SmpB_{His}$ protein to the acceptor-T arm was saturable with half-maximal binding at a free protein concentration of ∼100 nM. Exactly the same affinity was observed when binding between the acceptor-T arms derived from the *E. coli* $tRNA^{Ala}$ and *A. aeolicus* tmRNA and their homologous SmpB proteins was tested (not shown). These interactions were not weakened by removal of the CCA termini from the acceptor-T arm derivatives (Figure 9b). Similarly, replacement of the T loop by the UUCG tetraloop in the *A. aeolicus* acceptor-T arm did not weaken its interaction with both the *E. coli* and *A. aeolicus* SmpB proteins. In contrast, simultaneous removal of the 3′ CCA terminus and the T loop from the acceptor-T arm increased the affinity of the remaining double helix. The K_d for this interaction, as estimated from the gel mobility shift assay, was ∼20 nM. The latter finding indicated that SmpB is a

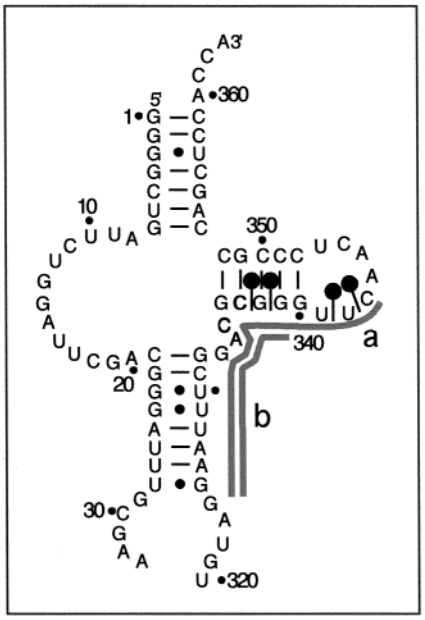

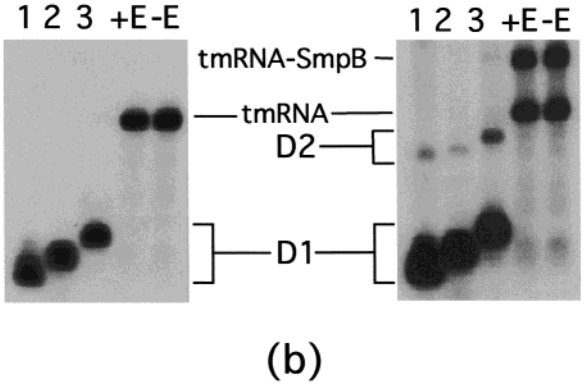

FIGURE 6: Localization of the cross-linked segment in the *E. coli* tmRNA by RNase H analysis. (a) The sites of hybridization of oligodeoxyribonucleotides "oligo a" and "oligo b" in the tRNA-like domain of the *E. coli* tmRNA. "Lollipops" indicate cleavages induced by RNase H. In the presence of "oligo c", RNase H cleaves tmRNA between residues 315 and 318 (not shown). (b) Autoradiograms of RNase H digests of 3′-^{32}P-labeled, UV-irradiated tmRNA (left) and covalent SmpB-tmRNA complexes (right) carried out in the presence of oligodeoxyribonucleotides oligo a (lane 1), oligo b, (lane 2) and oligo c (lane 3) and fractionated on a 10% polyacrylamide gel. D1 and D2 mark cleaved-off ^{32}P-labeled oligonucleotides and covalent oligonucleotide−SmpB complexes, respectively. Controls: +E, incubation with RNase H in the absence of oligodeoxyribonucleotides; -E, incubation without RNase H.

double-stranded RNA binding protein and that the T loop in both tmRNA and tRNA may negatively modulate this interaction. Moreover, this finding suggested that the same double helical motif may be recognized by the SmpB protein in the anticodon-like arm in tmRNA and in the anticodon arm of the tRNA molecule. Indeed, gel mobility shift assay showed that the anticodon arm analogue derived from *A. aeolicus* tmRNA and ending with tetraloop UUCG binds to SmpB proteins with K_d ∼100 nM (Figure 9c). We were, however, unable to determine whether removal of the tetraloop increases the affinity of the remaining helix for SmpB proteins because annealing of the gel-purified RNA

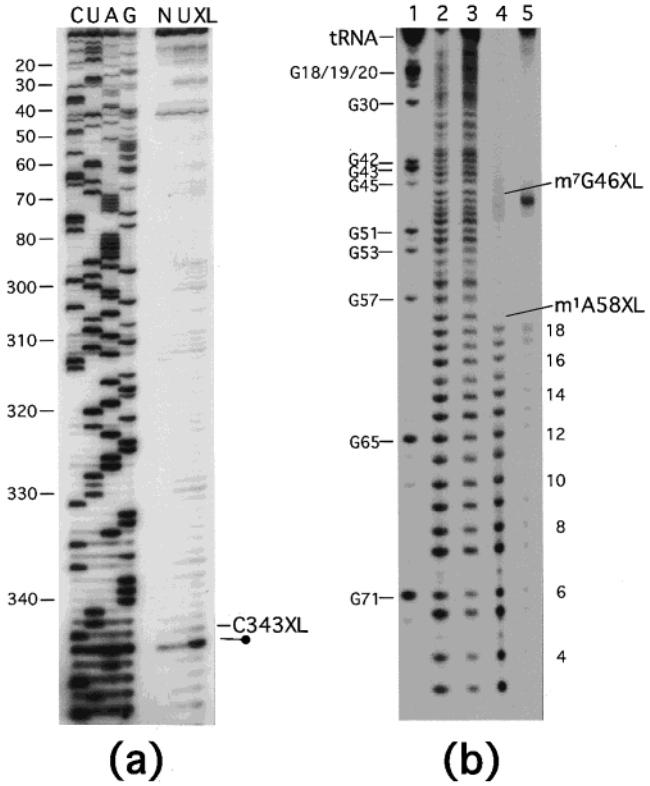

FIGURE 7: Identification of the nucleotides to which the *E. coli* protein $SmpB_{His}$ cross-links in *E. coli* tmRNA and yeast $tRNA^{Phe}$. (a) Primer extension analysis of cross-linked nucleotides in tmRNA−SmpB complexes in the presence of oligodeoxyribonucleotide complementary to nucleotides 352−363. The stop signal corresponding to the nucleotide preceding the cross-linked nucleotide C343 is indicated by a lollipop. N and U denote nonirradiated and UV-irradiated tmRNAs, respectively. XL denotes covalent tmRNA−SmpB complexes. C, U, A, and G are sequencing lanes. Numbers on the left side of the autoradiogram denote positions of nucleotides in the *E. coli* tmRNA. (b) Sequencing analysis of cross-linked nucleotides in tRNA−SmpB complexes according to Abdurashidova et al. (*35*). Lanes 1 and 2 are RNase T1 and alkaline ladders of 3′-^{32}P-labeled yeast $tRNA^{Phe}$. G residues and their numbers in the yeast $tRNA^{Phe}$ are on the left side of the autoradiogram. Lanes 3−5 show alkaline ladders of UV-irradiated 3′-^{32}P-labeled yeast $tRNA^{Phe}$, $tRNA^{Phe}$−SmpB, and $tRNA^{Phe}$−$(SmpB)_2$ complexes. Cross-linked residues m^7G46 and m^1A58 and the size of ^{32}P-labeled oligoribonucleotides that partitioned into aqueous phase are indicated on the right side of the autoradiogram.

strands produced heterogeneous duplexes. In addition, although enzymatic probing of tmRNA(Δ90−299)−SmpB protein complexes suggested that SmpB might interact with pseudoknot pk1 (Figure 9d), this interaction was not confirmed when binding of SmpB protein to a synthetic pseudoknot pk1 was tested by gel mobility shift assay.

DISCUSSION

The process of trans-translation, as suggested by Keiler et al. (*4*), could be divided into three phases. The first phase, initiation, begins when aminoacylated tmRNA binds to ribosomes stalled on mRNA and accepts an incomplete polypeptide from the P site-bound peptidyl−tRNA. During the next phase, elongation, a 10−27 amino acid-long peptide tag is synthesized according to the information encoded in the mRNA portion of tmRNA. The last phase, termination, begins when a stop codon marking the end of the mRNA domain in tmRNA enters the A site, a tagged protein is

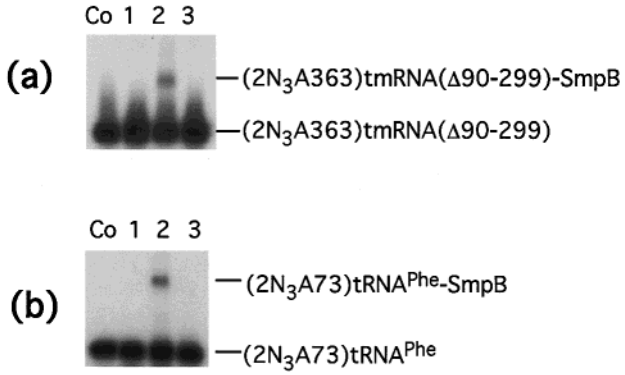

FIGURE 8: Affinity labeling of the *E. coli* $SmpB_{His}$ protein by $2N_3A$-substituted RNA ligands. (a) Formation of the covalent complexes between 3′-^{32}P-labeled $(2N_3A363)$tmRNA and SmpB protein by their irradiation with near-UV light. (Lane 1) Nonirradiated $(2N_3A363)$tmRNA, (lane 2) UV-irradiated $(2N_3A363)$tmRNA, (lane 3) UV-irradiated $(2N_3A363)$tmRNA−SmpB complexes, and (lane 4) UV-irradiated $(2N_3A363)$tmRNA−SmpB complexes treated with proteinase K. (b) Formation of the covalent complexes between 3′-^{32}P-labeled yeast $(2N_3A73)tRNA^{Phe}$ and SmpB protein by their irradiation with near-UV light. Lanes 1−4 as in panel a.

released and the ribosomes are recycled. Although tmRNA plays a central role in all three steps of trans-translation, its functions seem to depend on a number of proteins. As mentioned in the Introduction, three out of six proteins known to bind to tmRNA, either directly or through other proteins, are likely to help in binding tmRNA to stalled ribosomes. Recent and present studies have provided the first insight into the topography of the tmRNA complexes with EF-Tu, ribosomal protein S1, and SmpB protein (Figure 10a).

A compelling candidate for the role of trans-translational initiation factor is EF-Tu, which, together with GTP, facilitates binding of aminoacylated tRNA to the A site of the ribosome in the elongation stage of protein synthesis. Although the topography of the alanyl-tmRNA:EF-Tu:GTP complex has not yet been fully investigated, one could expect that as in tRNA, EF-Tu recognizes the acceptor-T arm (*49*). This suggestion is strongly supported by observations that aminoacylation is required for binding tmRNA to ribosomes in vivo and that only aminoacylated tmRNA and tmRNA-(Δ90−299) could bind to EF-Tu:GTP complex in vitro (*19*, *20*).

Another candidate for the trans-translational initiation factor is ribosomal protein S1. This protein may be found both on the ribosome and in the cytoplasm. A number of studies indicate that during protein synthesis protein S1 brings mRNA lacking the strong Shine−Dalgarno sequence into the proximity of the ribosomal decoding center and enhances the fidelity of the elongation step of protein synthesis (*50*). These functions are consistent with the location of protein S1 at the junction of the head, platform and main body of the 30S ribosomal subunit (*51*). In earlier studies (*22*), we demonstrated that ribosomes depleted of protein S1 are unable to bind tmRNA. Structural analysis of tmRNA-protein S1 complexes revealed that protein S1 interacts exclusively with the mRNA-like domain and pseudoknots pk2 and pk3 in the *E. coli* tmRNA. Taking into account the possibility that S1 disrupts helical regions of mRNAs (*52*), the interaction of tmRNA with protein S1 may contribute to both initiation and elongation of trans-translation by exposing the sequence preceding the "resume" codon and

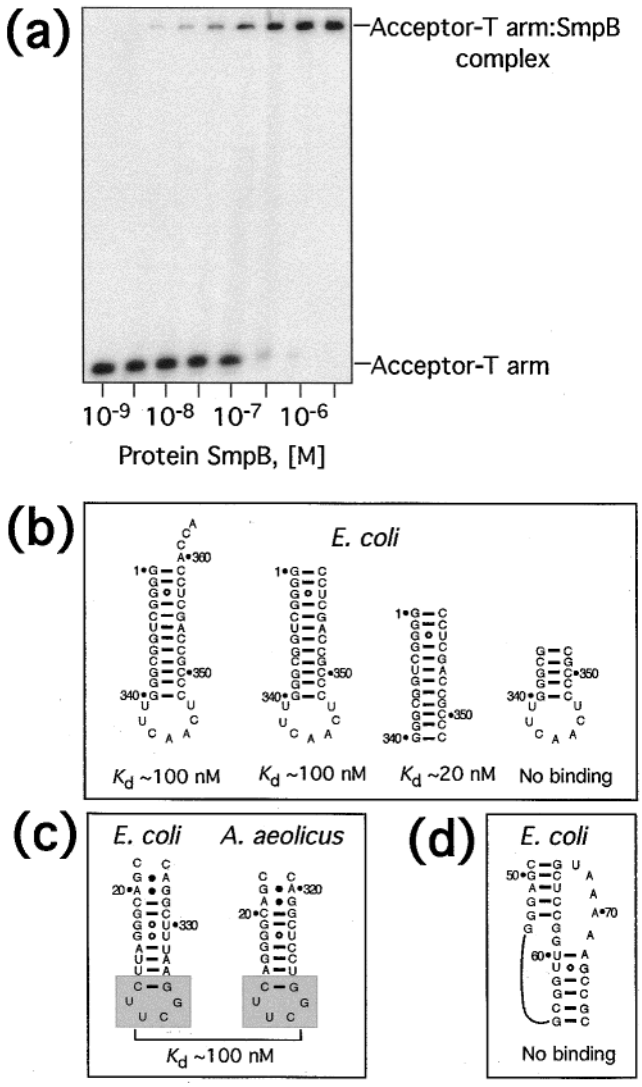

FIGURE 9: Binding of the *E. coli* $SmpB_{His}$ protein to synthetic fragments of the tmRNA molecule. (a) Titration of the 3′-^{32}P-labeled acceptor-T arm derived from the *E. coli* tmRNA with the *E. coli* $SmpB_{His}$ protein. (b) Synthetic derivatives of acceptor-T arm, (b) anticodon-like arm, and (c) pseudoknot pk1 tested for their binding affinity to the *E. coli* $SmpB_{His}$ protein. The K_d values determined by the gel mobility shift assays are indicated below the RNA structures.

by the optimizing interactions between anticodons of tRNAs and codons of the mRNA-like domain in tmRNA, respectively.

The third candidate for the trans-translational initiation factor, the SmpB protein, is present in all bacteria. Deletion of the *smpB* gene from *E. coli* abolishes peptide tagging because, as recently demonstrated by Shimizu and Ueda (*24*), in the absence of SmpB protein tmRNA is unable to bind to the A site of the stalled ribosome. In vitro, SmpB protein binds strongly to tmRNA (*27*), and recent studies by Barends et al. (*20*) demonstrated that SmpB, protein S1, and EF-Tu could bind to tmRNA simultaneously. This finding suggests that the binding sites for these three protein molecules do not overlap.

To determine the topography of SmpB binding sites on tmRNA, we chose four complementary approaches, gel mobility shift assay, enzymatic footprinting, UV-induced RNA-protein cross-linking, and affinity labeling. Our preliminary binding experiments demonstrated that SmpB protein preferentially binds to RNAs containing double-stranded regions. In tmRNA(Δ90−299), the sites to which SmpB binds are located outside the region that spans the mRNA domain and pseudoknots pk2, pk3, and pk4. Efficient competition between various tRNA and tmRNA(Δ90−299) suggested that SmpB specifically recognizes the tRNA-like domain of the tmRNA molecule. This observation was consistent with enzymatic probing of tmRNA−SmpB complexes, which demonstrated extensive protection of all parts of the tRNA-like domain of tmRNA except the D domain. Consistent with these observations was our finding that in vitro, tRNA could compete with tmRNA for the SmpB protein. Enzymatic footprinting of tRNA−SmpB protein complexes revealed that as in tmRNA, the acceptor-T, and anticodon arms were protected. Given that the SmpB proteins from *E. coli* and *A. aeolicus* are only approximately 50−60 Å in length (Figure 10b), enzymatic probing experiments suggested that at least two SmpB proteins could bind to each tmRNA and tRNA molecule. This suggestion was confirmed by cross-linking experiments, as UV irradiation of both tmRNA and tRNA in the presence of increasing amounts of SmpB protein revealed the formation of three types of covalently bound RNA-protein complexes.

As demonstrated by labeling the SmpB protein with $(2N_3A363)$tmRNA(Δ90−299) and $(2N_3A76)tRNA^{Phe}$ and cross-linking the SmpB protein to the C343 residue in the *E. coli* tmRNA and the m^1A58 residue in yeast $tRNA^{Phe}$, the first SmpB protein that binds to tmRNA and tRNA molecules attaches itself to their acceptor-T arms (Figure 10a,b). The acceptor-T arm is also a binding site for EF-Tu (*49*). However, mapping the phosphodiester bonds protected by SmpB on the three-dimensional structures of tRNA-like domain of *E. coli* tmRNA and yeast $tRNA^{Phe}$ revealed that most of the protection is afforded on the side that, as shown by crystallographic analysis of the ternary complex between Phe-$tRNA^{Phe}$, EF-Tu, and a GTP analogue (*49*), is not in contact with the EF-Tu molecule. Such an arrangement of the SmpB protein on the acceptor-T arm of tmRNA is consistent with the earlier finding that binding of a single SmpB molecule to alanyl-tmRNA does not interfere with the simultaneous binding of the latter molecule to the EF-Tu:GTP complex (*20*).

Although the CCA termini of tmRNA and tRNA are strongly protected by SmpB from degradation by nuclease S1 (this study) and RNase A (*20*), they are dispensable for SmpB interactions with both RNA molecules, as exemplified by the similar binding affinities of an intact acceptor-T arm and its truncated derivative lacking the 3′ terminal ACCA sequence to the SmpB protein and by the labeling of SmpB protein by $(2N_3A73)tRNA^{Phe}$ lacking a CCA terminus. This observation is not surprising, given that earlier studies demonstrated that aminoacylation of tmRNA is not required for its interaction with the SmpB protein (*27*). In contrast, as indicated by a number of studies including X-ray crystallography, the 3′ CCA terminus and its attached aminoacyl moiety are essential for the formation of the ternary complex between aminoacylated tRNA, EF-Tu, and GTP (*49*). Structural differences between the SmpB:acceptor-T arm complexes and ternary complex are further highlighted by the inability of the SmpB protein to bind to the T arm analogue, which together with the aminoacylated 3′ CCA sequence and the 5′ residue constitute the binding site of

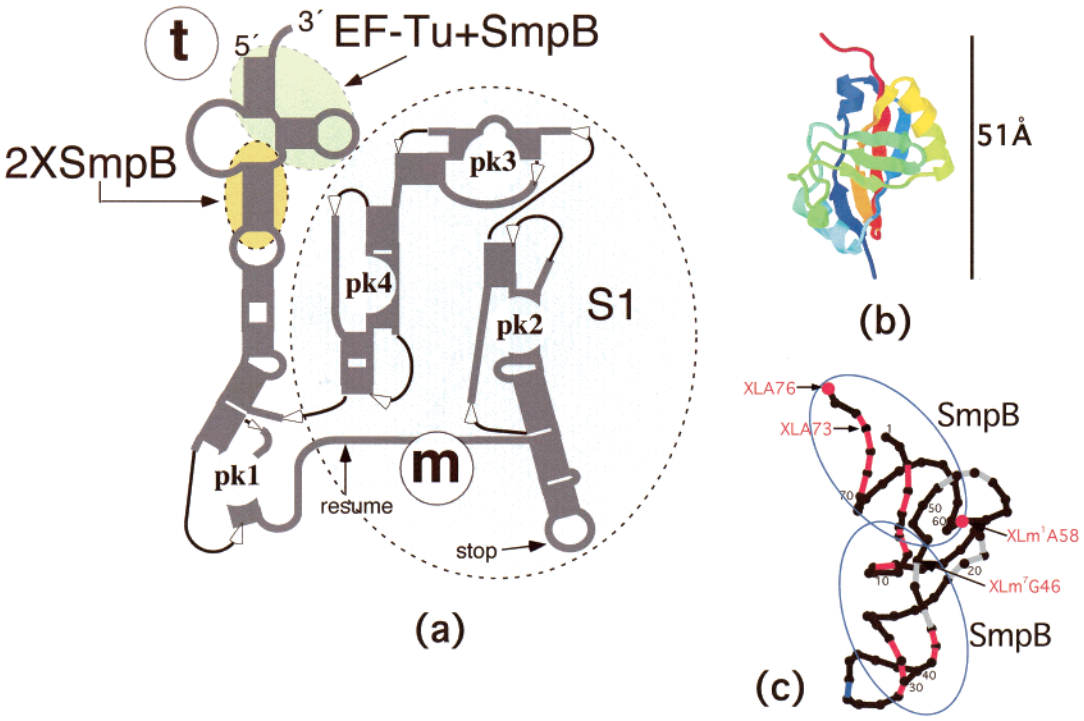

FIGURE 10: Topography of the tmRNA- and tRNA-protein complexes. (a) Distribution of binding sites for EF-Tu, ribosomal protein S1, and SmpB protein in *E. coli* tmRNA. The mRNA, tRNA-like domains, and pseudoknots are marked m, t, and pk, respectively. (b) Three-dimensional structure of the *A. aeolicus* SmpB(Δ134−157) (PDB entry number 1K8H) determined by Dong et al. (27). The length of the protein (51 Å) is indicated by the bar. (c) Distribution of SmpB protein binding sites in yeast $tRNA^{Phe}$. Gray and red lines denote phosphodiester bonds not protected and protected by SmpB protein from RNase degradation. Ovals mark suggested arrangement of SmpB protein molecules on tRNA. Xlm^1A58, XLA73, and XLA76 denote nucleotides cross-linked to the SmpB protein.

the EF-Tu:GTP complex (*49*). Therefore, unlike EF-Tu, SmpB appears to be a protein that specifically targets double-stranded RNA segments. However, its binding to double-stranded RNA is likely to be negatively modulated by such single-stranded RNA motifs as loops and bulges. This property is exemplified by the observation that removal of the T loop from the acceptor-T arm increases the affinity of the remaining double-helix for SmpB protein. It is possible that because of the difference in the accessibility of T loops in tmRNA and tRNA, SmpB stimulates the efficiency of alanylation of tmRNA and inhibits it in tRNA (*20*).

The high binding affinity of the SmpB protein with double-stranded RNA is consistent with its association with the anticodon arm-like segment in tmRNA and the anticodon arm in tRNA. Distribution of the protections given by SmpB protein in both tmRNA and tRNA, cross-linking of SmpB protein to nucleotides 330−335 in tmRNA and m^7G46 in the "extra arm" of yeast $tRNA^{Phe}$, and similar lengths of SmpB protein and its RNA ligands suggest that SmpB proteins could bind to the opposite sites of the helix. Although SmpB protein binds the synthetic analogue anticodon arm-like segment of tmRNA with the same affinity as the acceptor arm, in tmRNA and tRNA molecules, this interaction is weakened by the neighboring bulge and the anticodon loop. What role these two SmpB protein molecules play in tmRNA function is difficult to predict at present. It is possible that they provide additional protection against RNase degradation for the functionally important anticodon arm-like segment of tmRNA. Alternatively, assuming that SmpB has two functional RNA binding domains, these two proteins might contribute to the three-dimensional folding of the tmRNA molecule by interacting with pseudoknot pk1. Although we were not able to confirm an SmpB interaction with synthetic pseudoknot pk1, this suggestion is consistent with the protection extended by the SmpB protein, as demonstrated by enzymatic probing. Moreover, a long-range interaction between residues C44 and C66 suggests that in the three-dimensional structure of tmRNA, pseudoknot pk1 is located much closer to the tRNA-like segment than was anticipated by earlier studies (*15*, *16*).

Finally, our finding that SmpB is able to bind to at least some tRNA molecules opens the possibility that this protein also indirectly facilitates binding of tmRNA to ribosomes by lowering the aminoacylation efficiency of at least some tRNAs, thus preventing their binding to EF-Tu:GTP complexes. Given that formation of tRNA−SmpB protein complexes may have a detrimental effect on the elongation phases of trans-translation and protein synthesis, this process is likely to be regulated. Investigation of possible regulatory mechanisms is in progress.

ACKNOWLEDGMENT

We are grateful to Dr. J. Horowitz for expression plasmid for *E. coli* $tRNA^{Ala}$. We would also like to thank Dr. M. Kavousi for his help in the preparation of the *E. coli* SmpB protein.

REFERENCES

1. Karzai, A. W., Roche, E. D., and Sauer, R. T. (2000) *Nat. Struct. Biol. 7*, 449−455.
2. Wower, J., Zwieb, C., and Wower, I. K. (2000) in *The Ribosome: Structure, Function, Antibiotics, and Cellular Interactions* (Garrett, R. A., Douthwaite, S. R., Liljas, A., Matheson, A. T., Moore, P. B., and Noller, H. F., Eds.) pp 397−405, ASM Press, Washington, DC.

3. Wower, J., Wower, I. K., Kraal, B., and Zwieb, C. W. (2001) *J. Nutr. 131*, 2978S-2982S.
4. Keiler, K. C., Waller, P. R., and Sauer, R. T. (1996) *Science 271*, 990−993.
5. Roche, E. D., and Sauer, R. T. (1999) *EMBO J. 18*, 4579−4589.
6. Roche, E. D., and Sauer, R. T. (2001) *J. Biol. Chem. 276*, 28509−28515.
7. Keiler, K. C., Shapiro, L., and Williams, K. P. (2000) *Proc. Natl. Acad. Sci. U.S.A. 97*, 7778−7783.
8. De la Cruz, J., and Vioque, A. (2001) *RNA 7*, 1708−1716.
9. Williams, K. P., and Bartel, D. P. (1996) *RNA 2*, 1306−1310.
10. Felden, B., Himeno, H., Muto, A., McCutcheon, J. P., Atkins, J. F., and Gesteland, R. F. (1997) *RNA 3*, 89−103.
11. Zwieb, C., Wower, I. K., and Wower, J. (1999) *Nucleic Acids Res. 27*, 2063−2071.
12. Zwieb, C., Guven, S. A., Wower, I. K., and Wower, J. (2001) *Biochemistry 40*, 9587−9595.
13. Stagg, S. M., Frazer-Abel, A. A., Hagerman, P. J., and Harvey, S. C. (2000) *J. Mol. Biol. 309*, 727−735.
14. Hanava-Suetsugu, K., Bordeau, V., Himeno, H., Muto, A., Muto, A., and Felden, B. (2001) *Nucleic Acids Res.* 29, 4663−4673.
15. Zwieb, C., Müller, F., and Wower, J. (1999b) *Nucleic Acids Res. Symp. 41*, 200−204.
16. Kelley, S. T., Harris, J. K., and Pace, N. R. (2001) *RNA 7*, 1310−1316.
17. Spacciapoli, P., Doviken, L., Mulero, J. J., and Thurlow, D. L. (1989) *J. Biol. Chem. 264*, 3799−3805.
18. Shi, J.-P., and Schimmel, P. (1991) *J. Biol. Chem. 266*, 2705−2708.
19. Barends, S., Wower, J., and Kraal, B. (2000) *Biochemistry 39*, 2652−2658.
20. Barends, S., Karzai, A. W., Sauer, R. T., Wower, J., and Kraal, B. (2001) *J. Mol. Biol. 314*, 9−21.
21. Zvereva, M. I., Ivanov, P. V., Teraoka, Y., Topilina, N. I., Dontsova, O. A., Bogdanov, A. A., Kalkum, M., Nierhaus, K. H., and Shpanchenko, O. V. (2001) *J. Biol. Chem. 276*, 47702−47708.
22. Wower, I. K. Zwieb, C. W., Guven, S. A., and Wower, J. (2000) *EMBO J. 19*, 6612−6621.
23. Karzai, A. W., and Sauer, R. T. (2000) *Proc. Natl. Acad. Sci. U.S.A., 98*, 3040−3044.
24. Shimizu, Y., and Ueda, T. (2002) *FEBS Lett. 514*, 74−77.
25. Oh, B.-K., and Apirion, D. (1991) *Mol. Gen. Genet. 229*, 52−56.
26. Komine, Y., Kitabatake, M., Yokogawa, T., Nishikawa, K., and Inokuchi, H. (1994) *Proc. Natl. Acad. Sci. U.S.A. 91*, 9223−9227.
27. Karzai, A. W., Susskind, M. M., and Sauer, R. T. (1999) *EMBO J. 18*, 3793−3799.
28. Dong, G., Nowakowski, J., and Hoffman, D. W. (2002) *EMBO J. 21*, 1845−1854.
29. Wower, J., Hixson, S. S., and Zimmermann, R. A. (1989) *Proc. Natl. Acad. Sci. U.S.A. 86*, 5232−5236.
30. Liu, M., Chu, W. C., Liu, J. C., and Horowitz, J. (1997) *Nucleic Acids Res. 25*, 4883−4890.
31. Milligan, J. F., Groebe, D. R., Witherell, G. W., and Uhlenbeck, O. C. (1987) *Nucleic Acids Res. 15*, 8783−8798.
32. Monier, R., and Feunteun, J. (1971) *Methods Enzymol. 20*, 494−502.
33. Douthwaite, S., and Garrett, R. A. (1981) *Biochemistry 20*, 7301−7307.
34. England, T. E., Bruce, A. G., and Uhlenbeck, O. C. (1980) *Methods. Enzymol. 65*, 65−74.
35. Silberklang, M., Gilum, M. A., and RajBhandary, U. L. (1977) *Nucleic Acids Res. 4*, 4091−4099.
36. Christiansen, J., Egebjerg, J., Larsen, N., and Garrett, R. (1990) in *Ribosomes and Protein Synthesis. A Practical Approach* (Spedding, G., Ed.) pp 229−252, Oxford University Press, Oxford.
37. Wower, J., Hixson, S. S., and Zimmermann, R. A. (1988) *Biochemistry 27*, 8114−8121.
38. Abdurashidova, G. G., Tsvetkova, E. A., and Budowsky, E. I. (1989) *FEBS Lett. 243*, 299−302.
39. Sylvers, L. A., Wower, J., Hixson, S. S., and Zimmermann, R. A. (1989) *FEBS Lett. 245*, 9−13.
40. Schagger, H., and von Jagov, G. (1987) *Anal. Biochem. 166*, 368−379.
41. Dong, H., Nilsson, L., and Kurland, C. G. (1996) *J. Mol. Biol. 260*, 649−663.
42. Wikman, F. P., Siboska, G. E., Petersen, H. U., and Clark, B. F. C. (1982) *EMBO J. 1*, 1095−1100.
43. Dock-Bregeon, A.-C., Garcia, A., Giege, R., and Moras, D. (1990) *Eur. J. Biochem. 188*, 283−290.
44. Lowman, H. B. and Draper, D. E. (1986) *J. Biol. Chem. 261*, 5396−5403.
45. Wurst, R. M., Vournakis, J. N., and Maxam, A. M. (1978) *Biochemistry 17*, 4493−4499.
46. Horz, W., and Zachau, H. G. (1973) *Eur. J. Biochem. 32*, 1−14.
47. Brimacombe, R., Greuer, B., Gulle, H., Kosack, M., Mitchell, P., Osswald, M., Stade, K., and Stiege, W. (1990) in *Ribosomes and Protein Synthesis. A Practical Approach* (Spedding, G., Ed.) pp 131−159, Oxford University Press, Oxford.
48. Döring, T., Mitchell, P., Osswald, M., Bochkariov, D., and Brimacombe, R. (1994). *EMBO J. 13*, 2677−2685.
49. Nissen, P., Kjeldgaard, M., Thirup, S., Polekhina, G., Reshetnikova, L., Clarck, B. F. C., and Nyborg, J. (1995) *Science 270*, 1464−1472.
50. Subramanian, A. R. (1983) *Prog. Nucleic Acid Res. Mol. Biol. 28*, 101−142.
51. Sengupta, J., Agrawal, R. K., and Frank, J. (2001) *Proc. Natl. Acad. Sci. U.S.A. 98*, 11991−11996.
52. Bear, D. G., Ng, R., Derveer, D., Johnson, N. P., Thomas, G., Schleich, T., and Noller, H. F. (1976) *Proc. Natl. Acad. Sci. U.S.A. 73*, 1824−1828.

BI0201365